2018 Building Performance Analysis Conference and
SimBuild co-organized by ASHRAE and IBPSA-USA
Chicago, IL
September 26-28, 2018

HEAT AND MASS TRANSFER ANALYSIS OF THE MICRO-POROUS MEMBRANE/PHASE CHANGE MATERIAL BASED ENERGY RECOVERY VENTILATOR

Mohammed Salman Mohiuddin[1], Weihuan Zhao[1,*]
[1]University of North Texas, Denton, TX
[*]Corresponding author: weihuan.zhao@unt.edu

ABSTRACT

The work aims to investigate a unique membrane-based energy recovery ventilator (ERV) system combined with phase change material (PCM) to efficiently recover thermal energy and moisture between the incoming air and exhaust air from the buidling to reduce the HVAC system load. Heat and mass transfer simulations were conducted for this ERV system under various air temperatures and flow regimes. It has been found that the membrane/PCM based ERV system can achieve sensible effectiveness (heat recovery) of 65% - 98% while latent effectiveness (moisture recovery) of 60% - 80%.

INTRODUCTION

Buildings as they are designed and used today, contribute to serious environmental and economic problems as they are energy-intensive.With the growing demand of energy worldwide, the expected decline of energy sources and their potential harmful effects on the environment especially the fossil fuels, tremendous amounts of efforts and research are in progress to make buildings more energy efficient. According to the US Energy Information Administration, 2012 Commercial Buildings Energy Survey, the energy consumed by central Heating, Ventilation and Air-Conditioning (HVAC) systems accounts for 40% of the total energy used by the building. In the buildings equipped with the central HVAC system, the envelope is becoming tighter and better-insulated. In this case, the energy consumption resulted by the ventilation can be much higher than that caused by the heat transfer through the building shell (Juodis et al. 2006). According to ASHRAE Standard 62.1 – 2016, adequate ventilation rates are essential in providing proper indoor air quality (IAQ). Higher ventilation rates improve the IAQ by diluting pollutants such as airborne particles and volatile organic compounds. On the other hand, studies have shown that higher ventilation rates increase the building energy consumption.A prominent approach to achieve energy efficiency is the use of ERV technology. (Simonson et al. 2010) investigated the impact of ERV on annual cooling and heating energy consumption by modeling a 10-storey office building in four American cities as representatives of major climatic condition. The principle of operation in ERV is the existence of temperature difference and the difference in water vapor content between the warm-humid outside air and cool exhaust air from the building. When these two air streams are separated by a barrier which can conduct heat and moisture, the temperature and water content would strive to level out by transferring the heat and water content from higher concentration to lower concentration. The medium acting as a barrier can be an enthalpy wheel, porous hydrophilic membrane, heat pipe and thin plates. A comprehensive review of ERV technology based on different types and flow arrangement was provided by (Mardiana-Idayu et al. 2012).

The use of membranes enables a passive ventilation technology in ERV in which a thin membrane layer which is vapor-permeable can effectively exchange both heat and moisture provided there exists a considerable amount of differential in temperature and humidity. A detailed heat and mass transfer model for an ERV with a porous hydrophilic membrane core was presented by (Zhang et al. 1999). As shown in Figure 1, membranes are arranged in cross-flow, parallel-flow and counter-flow to orient the separated air streams in specific directions. The effectiveness value calculated as the ratio of actual energy exchange to the maximum energy exchange can be used to quantify the performance of an ERV. The heat and mass exchange is depicted as sensible and latent effectiveness, respectively. Effectiveness value is highest in counter-flow arrangement and lowest in parallel-flow arrangement. Cross-flow arrangement allows for a perfect sealing thereby preventing any mixing between the air streams. (Yaïci et al. 2012) performed the CFD modeling of membrane-based ERVs to predict the effect of critical parameters on the effectiveness value. There has been a continuous development in finding new membrane materials that enhances the exchange of heat and humidity. (Liu et al. 2009) investigated the performance of several hydrophilic materials to select the materials that are the most suitable for performing heat and mass transfer

between the incoming and outgoing air streams in a building. Commonly used hydrophilic materials include metals, fibers, ceramics, zeolites and carbons. Thermal conductivity of a membrane does not play a significant role in heat conduction owing to the small thickness. However, capillary force and pore size influences the moisture diffusion in a large way. Moisture deposition increases with porosity and large pore size expedites the moisture transfer rate. However, the pore size is limited to avoid air diffusion between the two streams.

The idea of thermal energy storage using phase change material (PCM) in mechanical ventilation and free cooling has long been studied by various researchers. The efficient charging (freezing) and discharging (melting) of PCM is crucial in delivering the required energy storage. The use of PCM in ventilation system is most suitable when the diurnal and nocturnal temperatures facilitate the charging and discharging potential. For free cooling in buildings, any PCM with a melting temperature in the range of 24°C-30°C and the charging temperature in the range of 18°C-22°C is desirable. (Turnpenny et al. 2000) and (Turnpenny et al. 2001) studied the free cooling experiment by storing coldness of the night air in the PCM and discharging during the daytime by virtue of heat pipes embedded in PCM that enhance the heat transfer between air and PCM. A latent heat thermal energy storage (LHTES) system for Night Ventilation with PCM (NVP) was developed by (Yanbing et al. 2003). In this work at night, the outdoor cool air is blown through the PCM package bed system to charge coldness of air to PCM. During daytime, heat is transferred to LHTES system, and the coldness stored by PCM at night is discharged to the room. The air flow rate was controlled to meet different cooling load demand at daytime. PCM employed in buildings is mostly encapsulated to prevent leakage and mostly used in places such as air channels, building walls, ceiling & floors etc. PCM encapsulation has been done in many ways like flat plate encapsulation, tube encapsulation, metal ball encapsulation, PCM in aluminum pouches and graphite compounds, PCM in granules etc. (Cabeza et al. 2004) studied the experimental installation of flat plate encapsulated PCM in free cooling of buildings. Flat plate PCM encapsulation as shown in Figure 2 has the following advantages, (i) the melting and freezing process of a PCM on a plate surface is symmetric, (ii) heat transfer in the PCM can be controlled with the selected thickness of the encapsulation and (iii) high area to volume ratio of storage is obtained. An experimental setup for testing PCM–air real-scale heat exchangers was performed by (Lazaro et al. 2009) concluded that the design of heat exchangers is of paramount importance as the PCM has lower values of thermal conductivity. PCMs are classified as organic, inorganic and eutectic. Inorganic PCM has higher thermal conductivity and energy storage density but is limited in free cooling application due to its corrosiveness, supercooling issue and phase segregation during phase change. Organic PCM can be sub-divided into paraffin and non-paraffin, which is a viable option for free cooling applications due to the thermal and chemical stability. Eutectic mixtures of organic and inorganic PCMs can be used to obtain the desired melting point.

The work presented in this paper is aimed at **(1)** determining the performance of membrane-based quasi-counter-flow ERV using CFD modelling, and **(2)** studying the effect of encapsulated PCM in air ducts to realize the augment in energy savings when employed simultaneously with the membrane-based ERV. In this study, asymmetric porous membrane with finger-like macro-voids to enhance the moisture diffusivity (Zhang et al. 2008) had been considered in the numerical modeling of the membrane ERV. Polyvinylidene fluoride (PVDF) is used as the base raw material to develop the membrane with further treatments. The working principle of a counter flow and a quasi-counter-flow ERV is shown in Figure 3. A quasi-counter-flow configuration combines the advantage of cross-flow's simply sealing and counter-flow's high efficiency.

(Zhang et al. 2010) conducted heat and mass transfer analysis of quasi-counter-flow membrane energy exchanger and found that the effectiveness of the current arrangement lie between those for cross-flow and those for counter-flow arrangements. The flow can be divided distinctly into three zones: two cross-like zones and a pure counter-flow zone. The less the cross-like zones are, the larger the pure counter-flow zone is, and the greater the effectiveness. In this study, only the counter-flow section is considered owing to its greater influence on the effectiveness. The membrane parameters are listed below in Table 1. Commercially available organic paraffin-based PCM RT-24 manufactured by Rubitherm GmbH is used. The selected PCM has a melting point of 24°C and a range of 21°C-25°C for charging and discharging. The properties for the PCM are listed in Table 2. PCM encapsulated in flat steel plates was mounted in air duct parallel to each other as shown in Figure 4. The duct section containing PCM was arranged downstream of the ERV to realize the effect of PCM to further reduce the temperature of outdoor supply air once it passes through the counter-flow ERV. It has been observed that the sensible effectiveness was greatly

enhanced by virtue of PCMs and the latent effectiveness was increased due to the higher effective diffusion coefficient of the asymmetric membrane.

The uniqueness of this work is to develop a membrane-based ERV combined with PCM to significantly reduce the moisture content and heat from the incoming air for remarkable energy savings from the HVAC system.

Table 1 Membrane Parameters

DESCRIPTION	VALUE
Thickness (µm)	75.1
Open Porosity	0.75
Thermal Conductivity (W/m·K)	0.092
Diffusion Coefficient (m^2/s)	1.23×10^{-5}

Table 2 PCM Properties

DESCRIPTION	VALUE
Latent heat of fusion (kJ/kg)	160
Specific Heat Capacity (Both Phases) (J/kg·K)	2000
Thermal Conductivity (Both Phases) (W/m·K)	0.2
Density (Solid) (kg/m^3)	880
Density (Liquid) (kg/m^3)	760

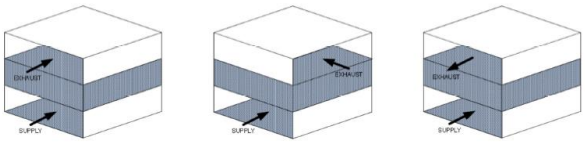

a) b) c)

Figure 1 Flow configurations in ERV. a) Parallel flow b) Cross flow c) Counter flow

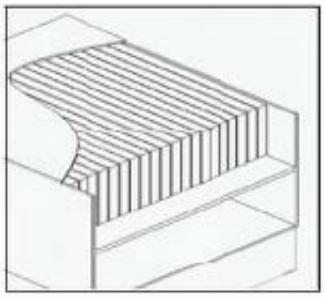

Figure 2 PCM Flat Plate Encapsulation (Cabeza et al. 2004)

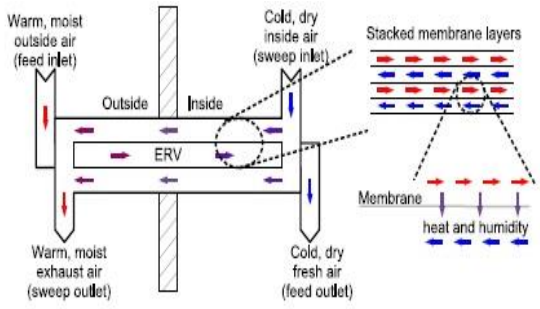

a)

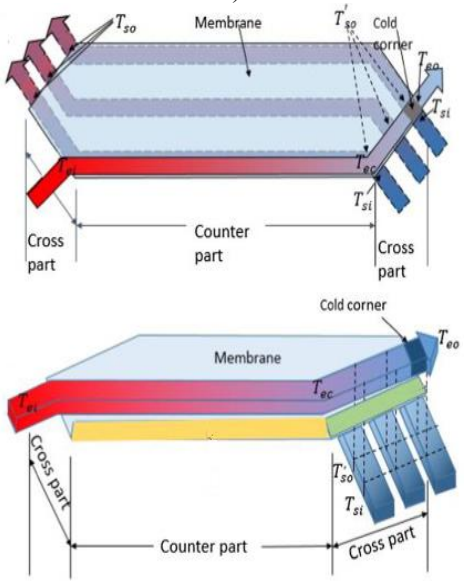

b)

Figure 3 Working Detail of a) Counter Flow ERV and b) Quasi-counter Flow ERV

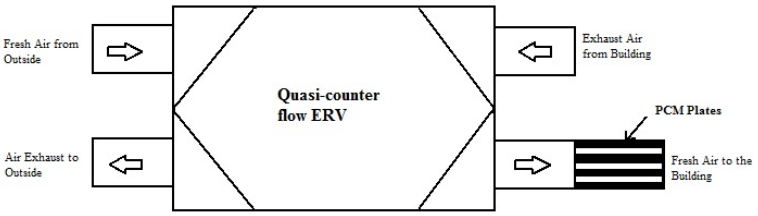

Figure 4 Schematic Layout of Quasi-Counter Flow ERV with PCM Plates

MEMBRANE ERV/PCM SIMULATION

Model Development for Membrane ERV

2D-models were developed for membrane ERV as shown in Figure 5 and the simulation was conducted in COMSOL Multiphysics. Conjugate heat transfer module

comprising of heat transfer and laminar flow in porous media were used. Based on the calculated Reynold's number (Re) value, the flow remained laminar for all the considered velocities. The mass transfer in porous media was accomplished using transport of diluted species module. Steady-state analysis was used to analyze the model. The porous membrane is sandwiched between the fresh air and exhaust air channels. The walls of the membrane were subjected to a no-slip boundary condition to prevent any air diffusion in the membrane and the outer planes of both the channels were given a symmetry boundary condition to save simulation time. The assumptions for the developed model include: i) air is incompressible, ii) membrane properties are homogeneous, iii) air streams do not cross the membrane, and iv) the air channels are perfectly insulated to avoid heat loss to the surrounding.

The governing equations used to model the fluid flow and heat and mass transfer are addressed as follows:

- Momentum equation:

$$\rho(u \cdot \nabla)u = \nabla \cdot [-p + \mu(\nabla u + (\nabla u)^{\mathrm{T}})] \quad (1)$$

- Continuity equation:

$$\rho \nabla \cdot (u) = 0 \quad (2)$$

- Energy equation:

$$\rho C_p u \cdot \nabla T + \nabla \cdot q = 0 \quad (3)$$

$$(q = -k_{eff} \nabla T\,; \quad k_{eff} = \theta_p k_m + (1 - \theta_p)k$$

- Mass transfer equation:

$$\nabla \cdot (-D_i \nabla C_i) + u \cdot \nabla C_i = 0 \quad (4)$$

Model Development for PCM in Duct Section

As depicted in Figure 5(b), the flat plate PCM encapsulations were arranged parallel to each other in a duct section through a 2D model. Conjugate heat transfer module comprising of heat transfer and laminar/turbulent flow was employed. The flow changed from laminar to turbulent with higher velocities. The interface between the air and PCM surface was subjected to a no-slip boundary condition and the outer surfaces of the duct section was subjected to symmetry condition to save the computational time. For this study, time-dependent analysis was employed for a period of 5 hours.

The governing equation to model the phase change process is expressed as follow:

$$\rho C_{p,PCM} \frac{\partial T}{\partial t} + \rho C_{p,PCM} u \cdot \nabla T + \nabla \cdot q = 0 \quad (5)$$

where $q = -k_{pcm} \nabla T$; $\rho = (\theta)\rho_{\ solid} + (1 - \theta)\rho_{\ liquid}$;

$C_{p,PCM} = C_{p,solid} + (C_{p,liquid} - C_{p,solid})B(T) + L\frac{d\alpha}{dT}$.

Here, the function of *B(T)* is the liquid fraction used to determine the change in the thermophysical properties between the solid and liquid phases of PCM (Samara et al. 2012; Zhao et al. 2014).

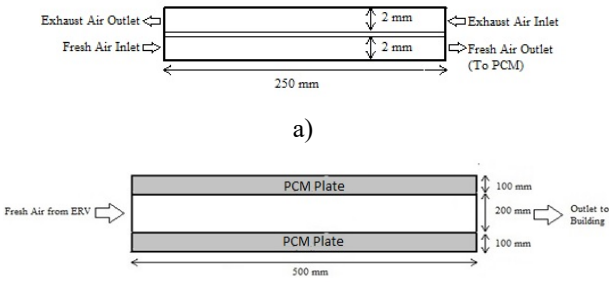

Figure 5 Developed 2D Models for a)Membrane ERV and b) Flat Plate PCM Encapsulations

Meshing

The mesh was created using triangular and quadrilateral elements. The overall mesh for membrane ERV contained 132,630 elements with a minimum element quality of 0.03273. The geometry for fresh air and exhaust air channels contained 49,506 and 49,406 elements respectively. The geometry for membrane domain consisted of 4,900 elements. Similarly, the model for flat-plate PCM encapsulation channel consisted of total 23,760 elements with a minimum element quality of 0.3968, including 9,556 elements for PCM domains and 18,674 elements for the fresh air channel. A mesh independence study was performed for both the models and verify the above mesh sizes are sufficient in this study.

RESULTS AND DISCUSSION

Inlet Parameters

The performance of the membrane ERV and the PCM plates was determined based on a parametric analysis. The study focuses on the energy savings potential during three summer months (June, July & August) for Denton, Texas. The outside air ambient temperatures for fresh air supply to the ERV were selected based on the design data for Dallas-Fort Worth (DFW) Intl. Airport, Texas available from ASHRAE (American Society of Heating, Refrigeration & Air-Conditioning Engineers). The inlet temperature of 33°C was selected as the average temperature in summer for Denton, Texas based on the Typical Meteorological Year 3 (TMY3) data for DFW Intl. Airport, Texas. Furthermore, another three temperatures (i.e., 36°C, 38°C, 40°C) were considered for the inlet according to ASHRAE design conditions,

which are encountered for the peak hours during the three summer months. The molar concentration remains the same as the relative humidity varies with temperature but not the absolte humidity. The study also involved varying inlet velocities, nevertheless, the inlet velocity for fresh air supply and exhaust air supply were identical at any instance. The values for data considered are as follows:

Fresh Air Inlet Temperature: 33°C; 36°C; 38°C; 40°C

Exhaust Air Inlet Temperature: 25°C

Initial Temperature: 22°C (This is the intial temperature of the entire system. For time-dependent study involving PCM, the initial temperature is expected be less than the melting point of the PCM.)

Inlet Velocities: 0.6 m/s; 1.25 m/s; 2.0 m/s

Absolute Humidity (molar concentration) at Fresh Air Inlet: 1.149 mol/m^3

Absolute Humidity (molar concentration) at Exhaust Air Inlet: 0.6507 mol/m^3

Impact of System Parameters on ERV Effectiveness

The performance of an ERV can be accurately described with effectiveness values. The greater the effectiveness, the higher the performance is for an ERV. In this study, the effectiveness values in regard to various velocities and inlet temperatures are studied. Moreover, the impact on effectiveness with the addition of PCM plates in the system is also realized. There are two measures for ERV effectiveness, the sensible effectiveness and the latent effectiveness. The sensible effectiveness is a ratio of the actual heat transfer to the maximum possible heat transfer. Similarly, the latent effectiveness is a ratio of the actual mass transfer to the maximum possible mass transfer. For an ERV in counter-flow configuration with the same flow rates and capacities of both the streams across the membrane, the sensible and latent effectiveness are given as:

$$\epsilon_s = \frac{T_{fi} - T_{fo}}{T_{fi} - T_{ei}} \quad (6)$$

$$\epsilon_l = \frac{C_{fi} - C_{fo}}{C_{fi} - C_{ei}} \quad (7)$$

A steady-state analysis of various air velocities and inlet temperatures on sensible effectiveness is performed and the effect of various air velocities on latent effectiveness is studied. Figure 6 and Figure 7 show the temperature profiles and concentration profiles respectively for different velocities considered.

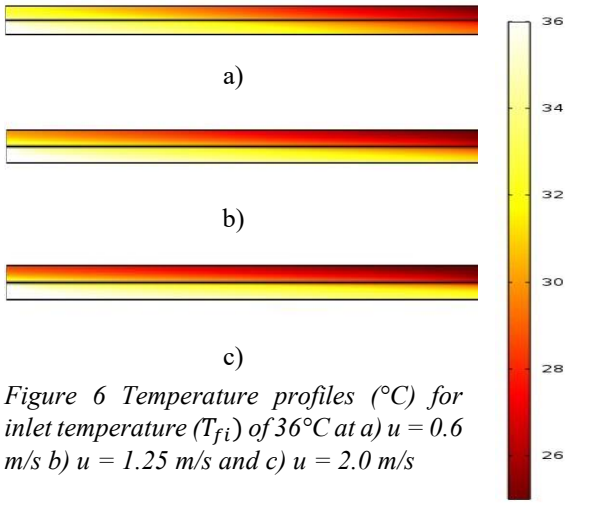

Figure 6 Temperature profiles (°C) for inlet temperature (T_{fi}) of 36°C at a) u = 0.6 m/s b) u = 1.25 m/s and c) u = 2.0 m/s

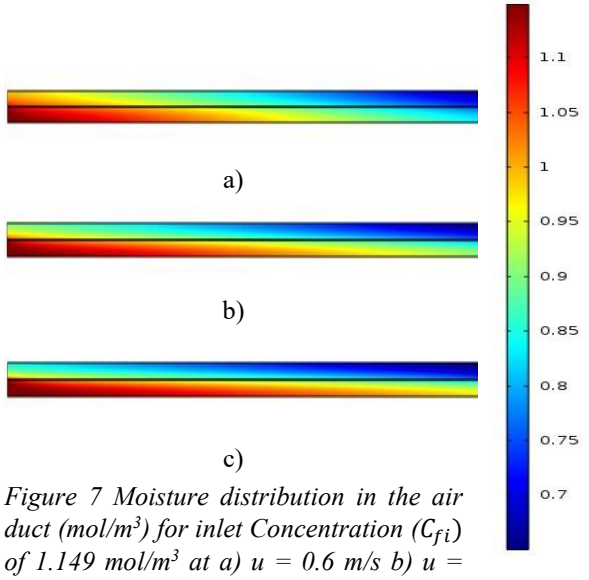

Figure 7 Moisture distribution in the air duct (mol/m^3) for inlet Concentration (C_{fi}) of 1.149 mol/m^3 at a) u = 0.6 m/s b) u = 1.25 m/s and c) u = 2.0 m/s

As depicted in the Figures 6 & 7, it can be noticed that the heat rate and mass transfer decreases with an increase in air velocity. Similar studies were conducted for inlet temperatures of 33°C, 38°C and 40°C while concentration at the inlet remaining the same in each case. The change in ERV sensible effectiveness for different air velocities and inlet temperatures is shown in Figure 8 while the change in ERV latent effectiveness for diffferent air inlet velocities is displayed in Figure 9.

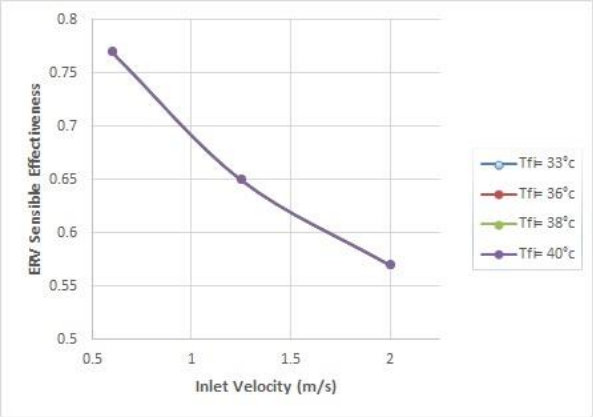

Figure 8 Change of ERV sensible effectiveness at various air inlet velocities and inlet temperatures

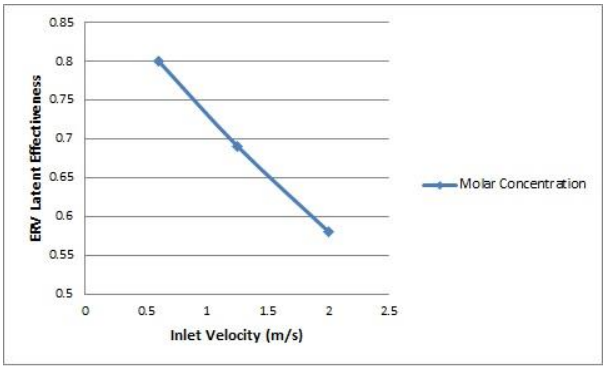

Figure 9 Change of ERV latent effectiveness at various air inlet velocities

It can be noted that the sensible effectiveness decreases with an increase in air velocity due to the decrease in actual heat transfer rate when compared to the maximum heat transfer rate. Moreover, the change in inlet temperature has no effect on the change in effectiveness values as the curve remains the same for all the four temperatures considered. The sensible effectivness at low inlet velocity is upto 77% while it stays at 57% at high inlet velocity. Also, the change in latent effectiveness follows a similar trend due to the decrease in mass transfer rate with increase in velocity. Because of the increased effective diffusivity with finger-like layers in the membrane, the latent effectiveness can reach 80% for lower velocities and maintains a decent 58% for higher velocities which is already much higher than other membranes. The simulaions conducted for a range of varying temperatures and water concentrations (absolute humidity) revealed that both sensible and latent effectivness values are unchanged for similar air inlet velocities.

Effect of PCM on System Effectiveness

The fresh air outlet temperatures from the ERV is further reduced by virtue of PCM encapsulated plates installed in the air duct downstream of the ERV which carries the fresh air to the occupied spaces in the building. The fresh air outlet temperature across various flow regimes and inlet temperatures serves as the entering temperature for the air channel containing the PCM plates as shown in Figure 5(b). Figure 10 shows the temperature profile for the air channel and the PCM temperature profile for different air flow rates. The inlet temperature to the air channel varies with velocity as it is the outlet temperature from the ERV. The system effectiveness in this case can be calculated as:

$$\epsilon_{s'} = \frac{T_{fi} - T_{fo'}}{T_{fi} - T_{ei}} \quad (8)$$

The air channel with PCM plates was subjected to a time-dependent analysis for the time range of 0-5 hours with an aim to study the decrease in temperature during peak hours. Figure 10 shows the temperature profiles for air channel and the PCM phase change for various airflow velocities (u). This figure is for the fresh air (from the outside environment) inlet temperature of 36 °C. The other air inlet temperatures of 33°C, 38°C and 40°C were also considered in this study.

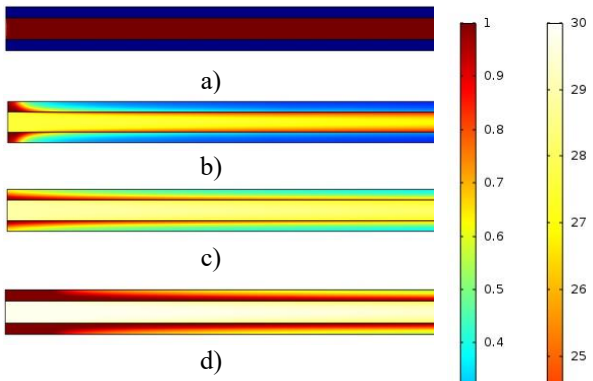

Figure 10 Temperature profiles (°C) for the air channel (right color legend) and PCM phase change (left color legend: 0 indicates pure solid state; 1 indicates pure liquid state) at a) t = 0 hour (the initial conditions) b) u = 0.6 m/s and t = 5 hours c) u = 1.25 m/s and t = 5 hours d) u = 2.0 m/s and t = 5 hours

The figure above shows that there is a considerable temperature drop of air across the air channel due to the melting of PCM. The inlet temperature for the PCM

embedded air channel in each case is not the same because the air source is from the exit of the ERV. It can be seen that the PCM melts largely with a higher airflow velocity, but the ability to decrease temperature across the channel remains nearly the same as that with low velocity because the temperature at the inlet of the channel (exiting temperature from the ERV) was increasing under high air velocity. The change of sensible effectiveness values by the PCM-embedded air duct is shown in Figure 11. The melted PCM can be solidified with night cooling during unoccupied hours when the ambient temperatures are below the melting point of the PCM.

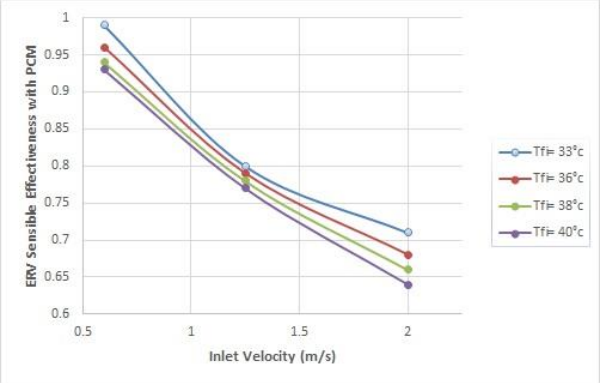

Figure 11 Change of sensible effectiveness in the PCM-embedded air channel under various air flow velocities

From the above figure, it is realized that the sensible effectiveness increases considerably with the addition of PCM plates downstream of the ERV. The time-dependent analysis of the PCM section revealed that the sensible effectiveness increases by more than 20% at lower air flow velocity and by around 15% at higher velocities resulting from the presence of PCM, which gives a great potential to decrease the cooling load during peak hours. It can also be inferred that the augmented effectiveness values increase with lower inlet temperatures as it causes the outlet temperature from the ERV to get close to the melting point of the PCM. However, there is a point at which lowering the temperature further will not have significant effect on the sensible effectiveness. The selection of PCM involves a range of temperatures and the air velocities for which it can work efficiently. When the temperatures are lower with lower airflow velocities such that they are less than or equal to the melting point of the PCM, the melting will not be initiated thereby not causing any temperature reductions. Conversely, when the temperatures are much higher with higher airflow velocities, the PCM will melt quickly, and therefore, the effect of temperature reduction by PCM cannot be utilized to the fullest extent.

Nomenclature

C_{ei}	Exhaust air inlet absolute humidity	mol/m^3
C_{fi}	Fresh air inlet absolute humidity	mol/m^3
C_{f0}	Fresh air outlet absolute humidity	mol/m^3
C_i	Concentration of water (humidity)	mol/m^3
C_p	Specific heat capacity	J/kg·K
$C_{p,liquid}$	Specific heat of liquid phase PCM	J/kg·K
$C_{p,pcm}$	Specific heat capacity of PCM (both phases)	J/kg·K
$C_{p,solid}$	Specific heat of solid phase PCM	J/kg·K
D_i	Diffusion coefficient	m^2/s
k	Thermal conductivity	W/m·K
k_{eff}	Effective thermal conductivity	W/m·K
k_m	Membrane thermal conductivity	W/m·K
k_{pcm}	PCM thermal conductivity	W/m·K
L	Latent heat of fusion	kJ/kg
q	Heat transfer rate	W
T	Temperature	K
T_{ei}	Exhaust air inlet temperature	°C
T_{fi}	Fresh air inlet temperature	°C
T_{f0}	Fresh air outlet temperature	°C
$T_{fo'}$	Fresh air outlet temperature with PCM	°C
t	Time	s
u	Velocity	m/s
Greek symbols		
ϵ_l	Latent effectiveness	
ϵ_s	Sensible effectiveness	
$\epsilon_{s'}$	Sensible effectiveness with PCM	
θ	Volume fraction of solid phase PCM	
θ_p	Volume fraction of membrane material	
μ	Dynamic viscosity	Pa-s
ρ	Density	kg/m^3
ρ_{liquid}	Density of PCM (liquid phase)	kg/m^3
ρ_{solid}	Density of PCM (solid phase)	kg/m^3

$\partial\alpha/\partial T$	Gaussian function used to account for the latent at of fusion	

CONCLUSION

The study revealed that the use of high-effective-diffusivity micro-porous membrane with finger-like layers is efficient in decreasing the incoming air humidity before it enters the building. The sensible effectiveness obtained were equivalent to other membranes being employed today, but the latent effectiveness (moisture recovery) was increased up to 80% due to the enhanced diffusivity. Through the modeling of the PCM plates downstream of ERV, it was found that PCM plates were highly effective in absorbing excess temperature of fresh air once it leaves the ERV. The sensible effectiveness (temperature reduction) increased by 15% - 22% due to the addition of PCM. Furthermore, the results show that the PCM in the plates is capable of the incoming air temperature reduction for up to 5 hours during the day time. The molten PCM can be retrieved during night through the solidification process. The future work in this study involves the determination of the amount of potential energy savings of building by performing a detailed energy analysis using a building energy simulation program.

ACKNOWLEDGMENT

This work was supported by University of North Texas, College of Engineering, Department of Mechanical and Energy Engineering Faculty Startup Fund.

REFERENCES

Cabeza, Luisa F., Marín, José M., Mehling, Harald, Zalba, Belén 2004. Free-cooling of buildings with phase change materials, International Journal of Refrigeration.

Juodis, Egidijus 2006. Extracted ventilation air heat recovery efficiency as a function of a building's thermal properties, Energy and Buildings.

Lazaro, Ana, Dolado, Pablo, Marin, Jose M., Zalba, Belen 2009. PCM–air heat exchangers for free-cooling applications in buildings: Experimental results of two real-scale prototypes, Energy Conversion and Management.

Liu, S., Zhao, X., Riffat, S., Yuan, Y. 2009. Comparative study of hydrophilic materials for air-to-air heat/mass exchanger, International Journal of Low-Carbon Technologies.

Mardiana-Idayu, A., Riffat, S.B. 2012. Review on heat recovery technologies for building applications, Renewable and Sustainable Energy Reviews.

Samara, F., Groulx, D., Biwole, P.H., 2012. Natural convection driven melting of phase change material: comparison of two methods. In: Proceedings of the 2012 COMSOL Conference in Boston.

Simonson, Carey J., Rasouli, Mohammad, Besant, Robert W. 2010. Applicability and optimum control strategy of energy recovery ventilators in different climatic conditions, Energy and Buildings.

Turnpenny, J.R., Etheridge, D.W., Reay, D.A. 2000. Novel ventilation cooling system for reducing air conditioning in buildings. Part I: testing and theoretical modelling, Applied Thermal Engineering.

Turnpenny, J.R., Etheridge, D.W., Reay, D.A. 2001. Novel ventilation cooling system for reducing air conditioning in buildings. Part II: testing of prototype, Applied Thermal Engineering.

Yaïci, Wahiba, Ghorab, Mohamed, Entchev, Evgueniy 2009. Numerical analysis of heat and energy recovery ventilators performance based on CFD for detailed design, Applied Thermal Engineering.

Yanbing, Kang, Yi, Jiang, Yinping, Zhang 2001. Modeling and experimental study on an innovative passive cooling system—NVP system, Applied Thermal Engineering.

Zhang, L.Z., Jiang, Y. 1999. Heat and mass transfer in a membrane-based energy recovery ventilator, Journal of Membrane Science.

Zhang, Li-Zhi, 2010. Heat and mass transfer in a quasi-counter flow membrane-based total heat exchanger, International Journal of Heat and Mass Transfer.

Zhang, Li-Zhi, 2009. Coupled heat and mass transfer through asymmetric porous membranes with finger-like macrovoids structure, International Journal of Heat and Mass Transfer.

Zhao, W., France, D.M., Yu, W., Kim, T., Singh, D., 2014. Phase change material with graphite foam for applications in high-temperature latent heat storage systems of concentrated solar power plants. Renewable Energy 69, 134–146.